

⁶V. Heine and R. O. Jones, *J. Phys. C: Proc. Phys. Soc.*, London **2**, 719 (1969).

⁷E. Loh, *Solid State Commun.* **2**, 269 (1964).

⁸J. T. Law, *J. Appl. Phys.* **32**, 848 (1961).

⁹W. Shockley, *Phys. Rev.* **56**, 317 (1939).

¹⁰R. O. Jones, *Phys. Rev. Lett.* **20**, 992 (1968); F. Yndurain, to be published.

¹¹M. Henzler, *J. Appl. Phys.* **40**, 3758 (1969).

¹²F. G. Allen and G. W. Gobeli, *Phys. Rev.* **127**, 150 (1962).

Spin-Wave Dispersion Relation in Dysprosium Metal*

R. M. Nicklow, N. Wakabayashi, M. K. Wilkinson, and R. E. Reed
Solid State Division, Oak Ridge National Laboratory, Oak Ridge, Tennessee 37830
 (Received 4 November 1970)

The spin-wave dispersion relation for the c direction of dysprosium metal in the ferromagnetic phase at 78°K and in the helical magnetic phase at 98°K has been measured by triple-axis neutron spectrometry. The energy gap measured in the ferromagnetic phase at $\vec{q}=0$ is in poor agreement with that calculated from the macroscopic magnetostriction and crystal-field anisotropy constants. The Fourier-transformed exchange interaction $J(\vec{q})-J(0)$ in the ferromagnetic phase possesses a peak near the wave vector that gives the periodicity of the helical structure just above the Curie temperature.

The spin-wave dispersion relation for the c direction of dysprosium metal in its ferromagnetic phase at 78°K and in its helical magnetic phase at 98°K has been measured by triple-axis neutron spectrometry. The measurements were carried out on the neutron spectrometer located at the Oak Ridge High Flux Isotope Reactor. Neutrons with energies in the range 10-16 meV were used. In addition to the usual constant- \vec{q} and constant- E modes of operation, numerous mixed scans (both q and E varied) were employed. The specimen is a single crystal grown in this laboratory of dysprosium enriched (96.8%) in the low-neutron-capturing isotope ^{163}Dy , and it weighs approximately 28 g. The neutron-capture cross section at 1 Å is estimated to be 100 b.

Dysprosium possesses a simple helical magnetic structure below T_N , 179°K, and a ferromagnetic structure below T_c , about 87°K.¹ Thus with dysprosium one has a unique opportunity to study

the exchange and anisotropy interactions over a relatively wide temperature range in both types of magnetic structures in the same metal. Of particular interest is the mechanism responsible for the magnetic phase transition and the extent to which the exchange interactions on either side of this transition differ. In the present Letter we report the results of measurements which were made primarily to examine the latter point.

The measured dispersion curves are shown in Figs. 1 and 2. For the ferromagnetic phase (78°K), the relative uncertainty of the measurements is estimated to be ~0.02 meV at small q and ~0.05 meV near the zone boundary. For the helical phase the errors at present are generally larger (0.04-0.10 meV).

The interpretation of these data has been based on the frozen-lattice model which leads to the following expression for the magnon energies along the c axis in the ferromagnetic phase^{2,3} at $T=0^\circ\text{K}$:

$$\hbar\omega(\vec{q}) = S \left\{ [J(0) - J(\vec{q}) + 2P_2 S(\frac{1}{2})/S^2] [J(0) - J(\vec{q}) + C\gamma(\lambda\gamma)^2/S^2 + 36P_6 S(\frac{5}{2})/S^2] \right\}^{1/2}, \quad (1)$$

with

$$S(n) = S(S - \frac{1}{2})(S - 1) \cdots (S - n).$$

Here S is the total angular momentum on each ion; $J(\vec{q})$ is the Fourier transform of the exchange interaction; P_2 and P_6 are the axial and hexagonal crystal-field anisotropy parameters; $\lambda\gamma$ is the parameter which specifies the lowest order single-ion magnetoelastic interaction, and $C\gamma$ is an elastic constant. The hexagonal anisotropy and magnetoelastic parameters usually occurring in the first bracket have been ignored here in comparison with P_2 .

The energy gap at $\vec{q}=0$ measured in the ferromagnetic phase is 1.40 ± 0.05 meV. From Eq. (1) this gap theoretically is given by

$$\hbar\omega(0) = S^{-1} \{ 3K_2 [36K_6 + C\gamma(\lambda\gamma)^2] \}^{1/2}, \quad (2)$$

where we have replaced P_2 and P_6 by the measured macroscopic anisotropy constants K_2 and

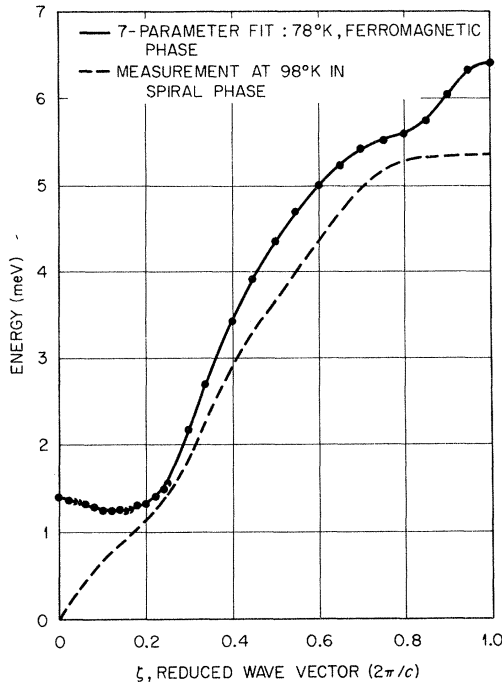


FIG. 1. The spin-wave energies measured in the c direction for ferromagnetic ^{163}Dy at 78°K , compared with the results obtained in the helical phase at 98°K .

K_6^6 . Using the experimental values (appropriate to 78°K) for anisotropy constants,⁴ the elastic constant,⁵ and the magnetostriction constants,⁶ one calculates 0.9 meV for the energy gap, which is in very poor agreement with the spin-wave measurement. If the $\sim 40\%$ larger value for K_6^6 as determined by Liu et al.⁷ is used, the calculated gap becomes 1.0 meV.

If one assumes that K_2 as measured by Rhyne and Clark⁴ is correct and that an effective planar anisotropy can be deduced from the measured energy gap, then the exchange function for the c direction $J(\vec{q})-J(0)$ can be determined directly from the measurements of $\hbar\omega(\vec{q})$. The results obtained are shown in Fig. 3. These results do not depend greatly on the detailed mechanisms responsible for the anisotropy so long as the discrepancy noted above is not due to a two-ion anisotropy which would then introduce an additional \vec{q} -dependent term into Eq. (1).

For wave vectors along the c axis the exchange function can be expressed as a cosine series with interplanar exchange constants as the coefficients, viz.

$$J(\vec{q})-J(0) = 2 \sum_l J_l [\cos(l\xi\pi) - 1], \quad (3)$$

with $|\vec{q}| = 2\pi\xi/c$ and $\xi \leq 1$. A linear least-squares fitting of Eq. (3) to the 78°K experimental results

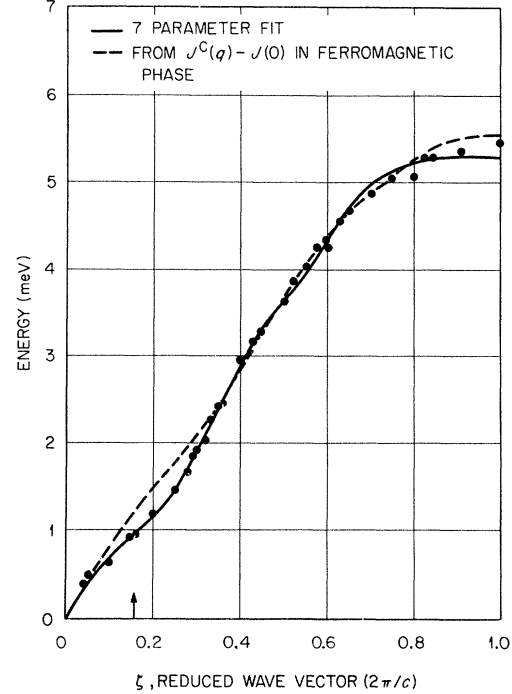


FIG. 2. The spin-wave energies measured in the c direction for ^{163}Dy in the helical phase at 98°K . The arrow denotes the helical wave vector \vec{Q} .

is shown in Fig. 3, and the exchange constants obtained are given in Table I. Seven constants are needed to fit the measurements of $J(\vec{q})-J(0)$ within the experimental error. On the basis of calculations carried out in conjunction with the fitting analysis, the uncertainties of these constants are estimated to be 2% for J_1 , 10% for J_2 to J_5 , and 40% for J_6 and J_7 . The dispersion relation $\hbar\omega(\vec{q})$ that is calculated with these constants is compared with the data in Fig. 1.

The maximum in $J(\vec{q})-J(0)$ near $\xi=0.15$ obviously follows directly from the minimum observed in the dispersion relation and it occurs at a value of ξ which coincides with the wave vector \vec{Q} of the helical structure just above T_c . This maximum indicates that even in the ferromagnetic phase the exchange interaction favors a helical structure, the ferromagnetic structure of Dy being stabilized by anisotropy forces, largely of magnetoelastic origin, which are in "competition" with the exchange.² Attempts have been made previously to relate known anisotropy interactions^{2,5,8} to the exchange energy difference ΔE_{ex} between the ferromagnetic phase $\vec{q}=0$ and the helical-magnetic phase $\vec{q}=\vec{Q}$, with $\Delta E_{ex} \approx S^2 [J(\vec{Q})-J(0)]$. The value calculated for ΔE_{ex} from the exchange function determined at 78°K is about 7 meV, which is considerably larger

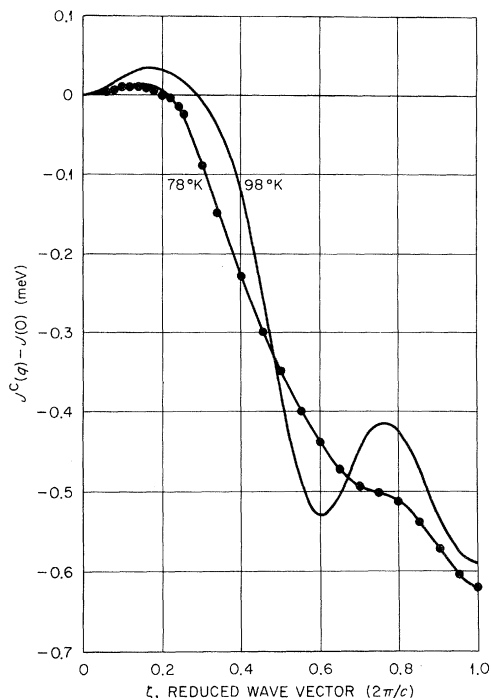


FIG. 3. The Fourier-transformed exchange in the c direction deduced for dysprosium from the spin-wave measurements in the ferromagnetic phase at 78°K and in the helical phase at 98°K.

than previous estimates of from 2 to 3 meV. Such an analysis, of course, ignores the possibility that the exchange interaction itself may be different in the two structures.

In the helical magnetic phase the γ -magneto-elastic strains vanish,⁸ and the basal plane anisotropy is averaged to zero. The magnon energies along the c axis are then

$$\hbar\omega(\vec{q}) = S \left\{ [J(\vec{Q}) - \frac{1}{2}J(\vec{Q}-\vec{q}) - \frac{1}{2}J(\vec{Q}+\vec{q})] \times [J(\vec{Q}) - J(\vec{q}) + 2B] \right\}^{1/2}, \quad (4)$$

where $S^2B = P_2S(S-\frac{1}{2})$. The experimental measurements obtained in the helical phase (see Fig. 2) are in rather good agreement with calculations based on the exchange function that was determined in the ferromagnetic phase, except near $\vec{q} \approx \vec{Q}$ where the calculation is $\sim 30\%$ too high. Again, we have used the macroscopic axial anisotropy constant.⁴ On the basis of Eq. (4) this discrepancy near \vec{Q} indicates that $J(\vec{Q})$ and/or $J(2\vec{Q})$ has changed significantly at the phase transition. An analysis of these data in terms of interplanar constants, as in Eq. (3), yields the constants given in Table I and an exchange function which is different at nearly all \vec{q} from that obtained in the ferromagnetic phase as illustrated in Fig. 3.

Table I. Interplanar exchange constants for dysprosium in the c direction, given in meV.

	Ferromagnetic phase (78°K)	Helical phase (98°K)
J_1	0.158	0.158
J_2	0.015	0.022
J_3	-0.005	-0.027
J_4	-0.017	-0.034
J_5	-0.001	0.024
J_6	-0.005	-0.001
J_7	0.004	-0.008

In particular, the peak $J(\vec{Q}) - J(0)$ is substantially larger, thereby suggesting an even larger ΔE_{ex} than that deduced from the ferromagnetic data. Obviously the comparison of the exchange energy of the two magnetic phases with various anisotropy energies either cannot be done in a molecular field theory or it should be based on the exchange in the helical phase, $J(\vec{Q})_H$, and the exchange in the ferromagnetic phase, $J(0)_F$. Apparently $J(0)_H \neq J(0)_F$.

Since a satisfactory analysis of the data in the helical phase can be achieved by using the macroscopic axial anisotropy constant, perhaps the discrepancy between the measured and calculated energy gap in the ferromagnetic phase is due to an error in the planar anisotropy interaction. Spin-wave measurements will be carried out soon at 4°K, where the anisotropy interactions are much larger, thereby producing a larger energy gap.

In the ferromagnetic phase the magnon dispersion relation crosses the longitudinal and transverse phonon branches in the c direction only at $\zeta \approx 0.05$ and $\zeta \approx 0.09$, respectively. Careful experimental examination of these crossing points revealed no detectable magnon-phonon interaction. However, when the temperature is lowered, the magnon dispersion curve will rise, and it then will intersect these phonon branches at additional points further out in the Brillouin zone. We expect magnon-phonon interactions to be detectable at these points as in the case for Tb.⁹

The authors wish to thank J. L. Sellers for his valuable technical assistance during this investigation.

*Research sponsored by the U. S. Atomic Energy Commission under contract with the Union Carbide Corporation.

¹M. K. Wilkinson, W. C. Koehler, E. O. Wollan, and J. W. Cable, J. Appl. Phys. Suppl. **32**, 485 (1961).

²B. R. Cooper, in *Solid State Physics*, edited by F. Seitz and D. Turnbull (Academic, New York, 1968), Vol. 21, pp. 393-490.

³M. S. S. Brooks, *Phys. Rev. B* **1**, 2257 (1970).

⁴J. J. Rhyne and A. E. Clark, *J. Appl. Phys.* **38**, 1379 (1967).

⁵M. Rosen and H. Klimker, *Phys. Rev. B* **1**, 3748 (1970).

⁶A. E. Clark, B. F. DeSavage, and R. Bozorth, *Phys. Rev.* **138**, A216 (1965).

⁷S. H. Liu, D. R. Behrendt, S. Legvold, and R. H. Good, Jr., *Phys. Rev.* **116**, 1464 (1959).

⁸W. E. Evenson and S. H. Liu, *Phys. Rev.* **178**, 783 (1969).

⁹M. Nielson, H. B. Møller, and A. R. Mackintosh, *J. Appl. Phys.* **41**, 1174 (1970).

M1 Transitions Among the $f_{7/2}d_{3/2}^{-1}$ States of $^{40}\text{K}^\dagger$

J. A. Becker

Lockheed Palo Alto Research Laboratory, Palo Alto, California 94304

and

E. K. Warburton

*Brookhaven National Laboratory, Upton, New York 11973, and
Lockheed Palo Alto Research Laboratory, Palo Alto, California 94304*

(Received 2 December 1970)

The three experimentally known $M1$ transition rates among the $f_{7/2}d_{3/2}^{-1} 2^-, 3^-, 4^-$, and 5^- quartet of ^{40}K are calculated to first order using the one-particle, one-hole wave functions of Perez. The calculations are in qualitative agreement with experiment and illustrate that the effective moment method is not valid when used with a zeroth-order (i.e., the pure $f_{7/2}d_{3/2}^{-1}$ configuration) calculation. This is expected since the effective moments correct for second-order effects and cannot simulate the first-order correction due to the presence of $f_{5/2}d_{3/2}^{-1}$ and $f_{7/2}d_{5/2}^{-1}$ impurities.

In two recent Letters^{1,2} mean lifetimes of the $M1$ transitions connecting the low-lying quartet of predominantly $f_{7/2}d_{3/2}^{-1}$ levels in ^{40}K have been measured and compared with shell-model predictions. Three $M1$ matrix elements are available for comparison: those corresponding to the $3^- \rightarrow 4^-$, $2^- \rightarrow 3^-$, and $5^- \rightarrow 4^-$ transitions. In the second of these studies² these matrix elements are compared with the predictions of a pure $f_{7/2}d_{3/2}^{-1}$ model and it is concluded that this model fails badly in predicting relative $M1$ transition rates, even if effective magnetic moments are used. In the first of these studies¹ small admixtures of $2p_{3/2}d_{3/2}^{-1}$ and $f_{7/2}2s_{1/2}^{-1}$ are included in the configuration space and effective moments are used. The agreement is then within a factor of about

2—which the authors consider good.

The purpose of this Letter is to point out that the most important impurities to be considered in calculating these $M1$ transitions are those which connect to the main term in first order—namely, those admixtures containing the other members of the $l_h \pm \frac{1}{2}$ and $l_p \pm \frac{1}{2}$ spin-orbit doublets. Furthermore, there is no reason to expect the effects of these admixtures to be simulated by effective moments since (1) they do not contribute in first order to the ^{39}K and ^{41}Ca magnetic moments, and (2) the force that generates them is not necessarily coherent with the $M1$ operator.

Let us consider in detail the three ^{40}K $M1$ rates which have been measured. We use the one parti-

Table I. Components $C_{j_p j_h}^J$ of the Perez particle-hole wave functions for the lowest four $T=1$ states of mass 40.^a

J^π	$1f_{7/2}1d_{3/2}^{-1}$	$1f_{7/2}1d_{5/2}^{-1}$	$1f_{5/2}1d_{3/2}^{-1}$	$1f_{7/2}2s_{1/2}^{-1}$	$2p_{3/2}1d_{5/2}^{-1}$	$1f_{5/2}1d_{5/2}^{-1}$	$2p_{3/2}1d_{3/2}^{-1}$	$2p_{3/2}2s_{1/2}^{-1}$
2^-	+0.959	+0.173	-0.087	...	+0.022	+0.072	-0.079	+0.173
3^-	+0.986	-0.080	-0.044	-0.131	+0.000	-0.007	-0.051	...
4^-	+0.995	+0.006	-0.012	+0.095	+0.011	+0.031
5^-	+0.991	-0.121	+0.050

^aThe phases are defined by the choices that $\vec{j}_p + \vec{j}_h = \vec{J}$, $\vec{l} + \vec{s} = \vec{J}$, and radial wave functions are positive at the origin.